



UDK: 530.12

**Dilraxon D. URINBOYEVA,**

PhD Student, Institute of Fundamental and Applied Research, "TIAME" National Research University

Tashkent, Uzbekistan

E-mail: dilrabokhon.rose@gmail.com, ORCID: 0009-0009-3019-3644

Reviewed by Bobir Toshmatov, Doctor of Physical and Mathematical Sciences (DSc), New Uzbekistan University.

## DYNAMICS AROUND SCHWARZSCHILD BLACK HOLE EMBEDDED IN THE DARK MATTER HALO

Annotation

In this paper, we construct a static, spherically symmetric black hole immersed in a Dehnen-  $(1, 4, \gamma)$  type dark matter halo. To explore the effect of the central core dark matter density on the dynamics around the black hole, we selected  $\gamma = -2$  the density near the centre remains significantly lower than other cases, confirming that dark matter has minimal presence in the central region.

**Key words:** spherically symmetric, black hole, dark matter, density

## ДИНАМИКА ВОКРУГ ШВАРЦШИЛЬДОВСКОЙ ЧЁРНОЙ ДЫРЫ, ВСТРОЕННОЙ В ГАЛО ТЁМНОЙ МАТЕРИИ

Аннотация

В данной работе мы строим статический, сферически симметричный чёрный дыр, погружённый в гало тёмной материи типа Дена-  $(1, 4, \gamma)$ . Чтобы исследовать влияние плотности тёмной материи в центральном ядре на динамику вокруг чёрной дыры, мы рассматриваем случай  $\gamma = -2$ , когда плотность вблизи центра остаётся значительно ниже по сравнению с другими сценариями, что подтверждает минимальное присутствие тёмной материи в центральной области.

**Ключевые слова:** сферически симметричный, чёрная дыра, тёмная материя, плотность

## QORONG‘I MODDA HALOSIDA JOYLASHTIRILGAN SCHWARZSCHILD QORA TUYNUGI ATROFIDAGI DINAMIKALAR

Annotation

Ushbu maqolada biz Dehnen-  $(1, 4, \gamma)$  turidagi qorong‘i materiya galaktikasi ichiga joylashtirilgan statik, sferik simmetrik qora tuynukni hosil qilamiz. Qora tuynuk atrofidagi dinamikaga markaziy yadroning qorong‘i materiya zichligining ta‘sirini o‘rganish uchun  $\gamma = -2$  holatda markaz yaqinidagi zichlik boshqa holatlarga nisbatan sezilarli darajada past bo‘lib qoladi, bu esa markaziy mintaqada qorong‘i materiyaning minimal darajada mavjudligini tasdiqlaydi.

**Kalit so‘zlar:** sferik simmetrik, qora tuynuk, qorong‘i materiya, zichlik

**Introduction.** Black holes generally located in dynamic environments where they interact with surrounding matter and gravitational fields. A Schwarzschild metric is then introduced to represent the black hole, but this method does not produce a fully consistent solution of Einstein’s equations, making it practical for galactic modeling but incomplete in the relativistic sense [1-4]. Konoplya and Zhidenko proposed a generalized formulation that derives exact solutions of Einstein’s equations accommodating various galactic energy–momentum tensor configurations. Alongside these relativistic models, several approximate frameworks have been suggested under additional astrophysical constraints and informed by observational data such as galactic rotation curves and supermassive black hole shadows [5-7]. This study examines a Schwarzschild black hole embedded in a Dehnen-  $(1, 4, \gamma)$  dark matter distribution.

**Background.** It is known that, Dehnen-  $(\alpha, \beta, \gamma)$  type dark matter distribution which is expressed as

$$\rho(r) = \rho_s \left( \frac{r_s}{r} \right)^\gamma \left[ 1 + \left( \frac{r_s}{r} \right)^\alpha \right]^{(\gamma-\beta)/\alpha} \quad (1)$$

The parameters and correspond to the central density and core radius of the dark matter halo, respectively. In this study, we focus on the specific model where  $\alpha = 1$  and  $\beta = 4$ . Regardless of the value of, the dark matter density profile follows a decay behaviour proportional to  $1/r^4$  at large distances. Fig.1 extends the analysis by considering  $\gamma = -2$  value. Here’s how the density profiles behave: Displays a density profile with a flatter distribution in small  $r_s / r$ , dark matter is less concentrated near the center. We can infer how changing  $\gamma$  affects astrophysical interactions, particularly black hole environments. Higher  $\gamma$  values lead to dense cores, which could significantly impact gravitational lensing, orbital stability, and accretion dynamics for :  $\gamma = -2$

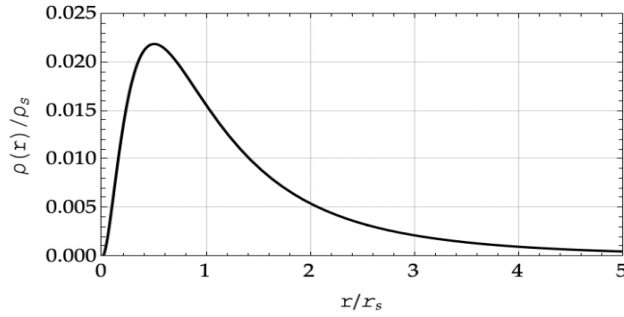


FIG. 1: The radial profile of the dark matter density

$$\rho(r) = \frac{r^2 r_s^4 \rho_s}{(r + r_s)^6} \quad (2)$$

To develop the spherically symmetric spacetime for pure dark matter, we apply the approach outlined in [8]. Assuming that the spacetime metric describing dark matter follows the given form, we proceed with its formulation accordingly.

$$ds^2 = -F(r)dt^2 + \frac{dr^2}{F(r)} + r^2 d\theta^2 + r^2 \sin^2 \theta d\phi^2 \quad (3)$$

On the equatorial plane  $\theta = \frac{\pi}{2}$ , the tangential velocity of the test particle is determined by

$$v_{ig}^2(r) = r \frac{d \ln \sqrt{F(r)}}{dr} \quad (4)$$

The tangential velocity of a particle following a circular trajectory within a dark matter spacetime is derived by analysing the mass distribution of the dark matter. This is expressed as:

$$v_{ig}^2 = M(DM) / r \quad (5)$$

$$M_{DM}(r) = 4\pi \int_0^r r'^2 \rho(r') dr' \quad (6)$$

To construct the dark matter spacetime, it is necessary to specify the explicit form of the density profile. As a particular case, we consider the dark matter spacetime

corresponding to the density profile given by (2). For this model, the dark matter mass distribution (7) and the tangential velocity are formulated as

$$M_{DM}(r) = \frac{4\pi \rho_s r_s^5 r^3}{5(r + r_s)^5} \quad v_{ig}^2(r) = \frac{4\pi \rho_s r_s^4 r^3}{5(r + r_s)^5} \quad (7)$$

$$F(r) = \exp\left(-\frac{2\pi r_s^3 (4r^3 + 6r^2 r_s + 4r r_s^2 + r_s^3)}{5(r + r_s)^4}\right) \quad (8)$$

We can write the spacetime geometry as:

$$ds^2 = -f(r)dt^2 + \frac{dr^2}{g(r)} + r^2 d\theta^2 + r^2 \sin^2 \theta d\phi^2 \quad (9)$$

Thus, for the dark matter density profile  $\gamma = -2$ , the metric function takes the following form:

$$f(r) = \exp\left(-\frac{2\pi r_s^3 (4r^3 + 6r^2 r_s + 4r r_s^2 + r_s^3)}{5(r + r_s)^4}\right) - \frac{2M}{r} \quad (10)$$

In order to write the exponential term in expression (10) in the rational expression form, we introduce characteristic mass of the core of the dark matter halo  $M_s = \pi \rho_s r_s^3$  and in terms of the small characteristic mass of the core of the dark matter halo relative to the mass of the black hole, i.e.,  $M_s / M \ll 1$ , we rewrite it as:

$$f(r) = 1 - \frac{2M}{r} - \frac{2\pi r_s^3 (4r^3 + 6r^2 r_s + 4r r_s^2 + r_s^3)}{5(r + r_s)^4} \quad (11)$$

When the characteristic mass of the dark matter halo's core is relatively small compared to the black hole's mass, the event horizon radius for these models can be expressed as:

$$r_H = 2M + \frac{8}{5} \pi r_s^3 \rho_s \quad (12)$$

Throughout the paper, our numerical computations treat the central dark matter density  $\rho_s \in [0,1]$  as a dimensionless quantity, normalized within the range, with the highest value set to one.

Accordingly, the dimensionless form of  $\rho_s$  is used only in plotting and computational assessments. For constraints involving the dark matter halo core mass, however,  $\rho_s$  is considered in its physical (dimensional) form. As illustrated in Fig. 2, the black hole's event horizon radius increases with higher values of both the core density and radius of the dark matter halo.

**Circular orbits.** This section examines the motion of a test particle in the vicinity of the black hole. To begin, we establish the equations governing the particle's motion. Due to the stationarity and spherical symmetry of the spacetime metric (11), certain components of momentum remain conserved. Specifically, the momenta associated with the temporal and azimuthal coordinates are constants of motion, corresponding to the particle's energy,  $E$ , and angular momentum,  $L$ , respectively.

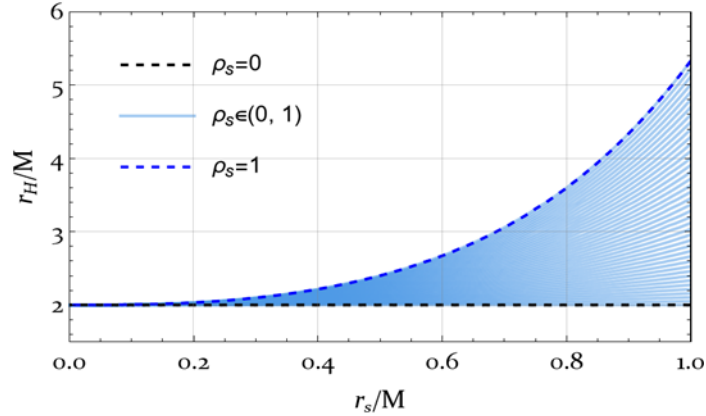


FIG. 2: The event horizon radius of the black hole in dark matter halo with dark matter density model and represented as a function of the halo core radius  $r_s$ . Halo core density values within the range specified in  $\rho_s \in [0,1]$ , varying in increments of 0.025.

$$u^t = \frac{E}{f(r)} \tag{13}$$

$$u^\phi = \frac{L}{r^2 \sin^2 \theta} \tag{14}$$

To streamline our calculations, we consider the test particle's motion to be restricted to the equatorial plane, where  $\theta = \pi/2$ . By applying the normalization condition for the 4-velocity, with  $u^\mu u_\mu = -\varepsilon$  taking a value of either unity for massive particles or zero for massless ones, we derive the corresponding expression for the particle's radial velocity.

$$(u^r)^2 = E^2 - V_{eff} \tag{15}$$

$$V_{eff} = f(r) \left( \frac{L^2}{r^2} + \varepsilon \right). \tag{16}$$

It is well established that a massive test particle ( $\varepsilon = 1$ ) traveling in a circular orbit within a central gravitational field experiences no radial velocity or radial acceleration. These constraints are mathematically formulated through the equations of motion as follows:

$$u^r = 0, \quad \frac{du^r}{d\tau} = 0. \tag{17}$$

By solving these equations simultaneously, one obtains the following expressions for the specific energy and angular momentum of the particle moving along the circular orbit:

$$E^2 = \frac{2f^2}{2f - rf'} \tag{18}$$

$$L^2 = \frac{r^3 f'}{2f - rf'} \tag{19}$$

By incorporating the metric functions (15), (16), and (17) into equations (18) and (19), one can derive explicit expressions for the specific energy and angular momentum of a particle in circular orbit around black holes influenced by dark matter models (2), (3), and (4). However, due to the complexity of these expressions, we do not present them explicitly here. To better illustrate the influence of dark matter on the specific energy and angular momentum—particularly in scenarios where the characteristic core mass of the dark matter halo is significantly smaller compared to the black hole's mass—we provide the energy as follows:

$$E = E_{Schw} + 0.8\delta E \tag{20}$$

$$L = L_{Schw} + 0.8\delta L \tag{21}$$

$$E_{Schw} = \frac{r - 2M}{\sqrt{r(r - 3M)}} \tag{22}$$

$$\delta E = -\frac{(r - 6M)M_s}{2\sqrt{r}(r - 3M)^{3/2}} \tag{23}$$

$$L_{Schw} = \frac{\sqrt{Mr}}{\sqrt{r - 3M}} \tag{24}$$

$$\delta L = -\frac{\pi\rho_s r^2 r_s^3}{2\sqrt{M}(r - 3M)^{3/2}} \tag{25}$$

Based on (24) and (25), within the interval  $3M < r < 6M$ , the presence of dark matter leads to an increase in the energy of a particle following a circular orbit. However, beyond  $r > 6M$ , this energy diminishes compared to its value in the vicinity of a Schwarzschild black hole. Despite this variation in energy, the particle's angular momentum consistently exhibits growth across these regions. The angular velocity of a particle in circular orbit, given by  $\Omega = u^\phi / u^t$ , can alternatively be represented in terms of components associated with the Schwarzschild black hole and the influence of dark matter.

$$\Omega^2 = \Omega_{Schw}^2 + 0.8\delta\Omega^2 \tag{26}$$

$$\Omega^2 = \frac{M}{r^3}, \quad \delta\Omega^2 = \frac{M_s r}{(r_s + r)^4} \tag{27}$$

$$\Omega_{GP} = \Omega\sqrt{f(r) - r^2\Omega^2} \tag{28}$$

As previously discussed [9], the spacetime line element (11) remains asymptotically flat across all the solutions analyzed in this work. Consequently, under the weak-field approximation, the geodetic precession frequency relative to distant stars can be expressed as  $\Theta_{GP} = \Omega - \Omega_{GP}$

$$\Theta_{GP} = \Theta_{GP}^{GR} - 0.8\delta\Theta \tag{29}$$

where,

$$\Theta_{GP}^{GR} = \frac{3M^{3/2}}{2r^{5/2}}, \quad \delta\Theta = \frac{9\sqrt{M}M_s}{4r^{5/2}} \tag{30}$$

The Gravity Probe B mission measured a precession rate of  $\Theta = -6601.8 \pm 18.3 \text{ mas/year}$ , while the theoretical value predicted by general relativity is  $\Theta_{GP}^{GR} = -6606.1 \text{ mas/year}$  [10]. Using the values  $r = (6371 + 642) \times 10^3 \text{ m}$ ,  $M_\otimes = 5.9722 \times 10^{24} \text{ kg}$ , we can constrain the characteristic mass of the dark matter halo core as  $M_s = \pi\rho_s r_s^3$ .

$$\Phi = \Phi^{GR} + 0.8\delta\Phi \tag{31}$$

where,  $\Phi^{GR} = \frac{3\pi M}{r} = 1.22943 \text{ mas}$  and  $\delta\Phi = \frac{3\pi M_s}{r}$  (32)

Consequently, the geodesic precession angle becomes independent of the dark matter models, falling within the specified range:

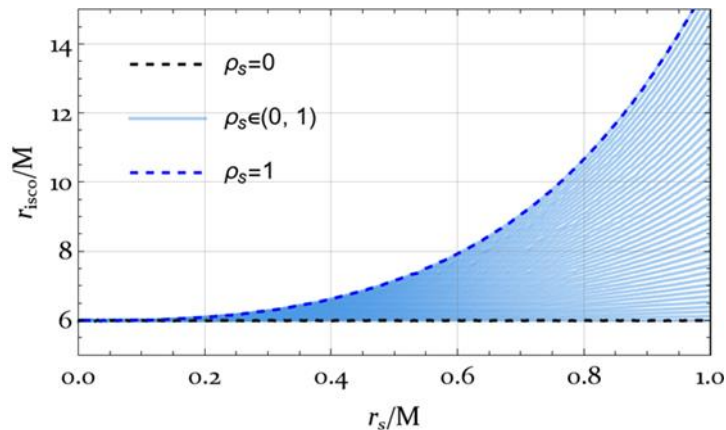


FIG. 3: The same as Fig.2, but for the ISCO radius.

$$1.22943 \text{ mas} \leq \Phi \leq 1.23116 \text{ mas}. \quad (33)$$

From the expressions for energy (25) and angular momentum (26), it is clear that circular orbits for a test massive particle are possible if the condition  $2f - f'' = 0$  is satisfied.

$$V_{\text{eff}}'' = 0 \quad (34)$$

The location of the ISCO for the black holes considered in this analysis cannot be derived using analytical techniques. Therefore, we rely on numerical methods to compute it, with the outcomes presented in Fig. 3 for the model under consideration. In line with previous studies, to evaluate the influence of the dark matter halo core radius on the ISCO radius, we calculate the ISCO radius assuming a small characteristic mass of the dark matter halo core in comparison to the black hole mass.

$$r_{\text{isco}} = 6M + \frac{24}{5} \pi \rho_s r_s^3, \quad (35)$$

**Conclusion.** In this study, we develop a static, spherically symmetric black hole model situated within a Dehnen-(1,4,  $\gamma$ ) type dark matter halo, characterized by a density profile that falls off as  $1/r^4$  at large radii. As noted in [11], the parameter  $\gamma$  is typically restricted to the interval  $[0, 3]$ , ensuring that the dark matter density diverges as  $1/r^4$  near the centre of the spacetime. To explore how the central density affects the dynamics around the black hole, we intentionally depart from this conventional range by choosing  $\gamma = -2$ , which yields a vanishing dark matter density at the core.

#### REFERENCES

1. Z. Xu, X. Hou, X. Gong, and J. Wang, JCAP 09, 038 (2018), arXiv:1803.00767 [gr-qc].
2. R. C. Pantig and A. Övgü'n, JCAP 08, 056 (2022),
3. C. Zhang, T. Zhu, X. Fang, and A. Wang, Phys. Dark Univ. 37, 101078 (2022), arXiv:2201.11352 [gr-qc].
4. A. Al-Badawi and S. Shaymatov, Communications in Theoretical Physics 77, 035402 (2025).
5. K. Boshkayev and D. Malafarina, Mon. Not. Roy. Astron. Soc. 484, 3325 (2019), arXiv:1811.04061 [gr-qc].
6. D. Liu, (2025), arXiv:2501.12213 [gr-qc].
7. D. Shadykul, H. Chakrabarty, and D. Malafarina, (2024), arXiv:2410.18657 [gr-qc].
8. T. Matos and D. Nunez, Rev. Mex. Fis. 51, 71 (2005), arXiv:astro-ph/0303594
9. B. Toshmatov and A. Abduraimov, Annals Phys. 440, 168845 (2022).
10. C. W. F. Everitt et al., Phys. Rev. Lett. 106, 221101 (2011), arXiv:1105.3456 [gr-qc].
11. C. W. Misner, K. S. Thorne, and J. A. Wheeler, Gravitation
12. W. H. Freeman and Company, San Francisco, 1973.